Acta Crystallographica Section A
Foundations of Crystallography
ISSN 0108-7673

Received 28 September 1999
Accepted 1 November 1999

© 2000 International Union of Crystallography
Printed in Great Britain – all rights reserved

Inversion of dynamical electron diffraction data including absorption

L. J. Allen,[a]* H. M. L. Faulkner[a] and H. Leeb[b]

[a]School of Physics, University of Melbourne, Parkville, Victoria 3052, Australia, and [b]Institut für Kernphysik, Technische Universität Wien, Wiedner Hauptstrasse 8-10/142, A-1040 Vienna, Austria. Correspondence e-mail: lja@physics.unimelb.edu.au

A method to invert the dynamical diffraction of high-energy electrons inside a crystal, which takes into account absorption, is discussed. It is shown that, working at fixed energy, the projected potentials associated with both the elastic and the absorptive scattering can be uniquely obtained from the scattering matrix. Inversion is possible for any principal orientation of the incident beam. Model examples are given.

1. Introduction

During the last two decades, considerable effort has been devoted to finding ways to retrieve not only the amplitude but also the phase of the complex wave function at the exit surface of a crystal in high-energy transmission electron diffraction. Holography (Lichte, 1991; Orchowski *et al.*, 1995) allows retrieval of the pertinent phase information, as does the information in a through-focus series of images (Kirkland, 1984; Tonomura, 1987; Van Dyck & Coene 1987; Lichte, 1991; Coene *et al.*, 1992; Gribelyuk & Hutchison, 1992; Van Dyck & Op de Beeck, 1993). Another approach, known as ptychography (from the Greek $\pi\tau\upsilon\xi$, meaning fold), is to determine the phase of the wave function *via* the interference patterns in overlapping convergent-beam electron diffraction (CBED) discs obtained using a coherent incident beam (Nellist *et al.*, 1995; Spence, 1998).

Attempts have been made to implement an inversion of the dynamical (multiple) scattering and recover the crystal structure (projected potential) from the exit-surface wave function for a single orientation of the incident beam (Gribelyuk, 1991; Beeching & Spargo, 1993; Peng & Wang, 1994; Dorset, 1995; Peng & Zuo, 1995; Gilmore, 1996; Lentzen & Urban, 1996; Van Dyck & Op de Beeck, 1996; Zou *et al.*, 1996; Zhu & Tafto, 1997), assuming that the space group of the lattice is known, *e.g.* by the method proposed by Zuo (1993). It has recently been pointed out (Allen *et al.*, 1999) that this problem is underdetermined, unless the crystalline slab is sufficiently thin. The scattering process is described by the $\mathcal{S}$ matrix, which relates the incident wave function (usually assumed to be a plane wave) to that at the exit surface of the crystal. The $\mathcal{S}$ matrix contains the information about the structure and the interactions within the crystal *via* the Bethe or structure matrix $\mathcal{A}$ in a nonlinear way. In general, because of this nonlinearity, an unambiguous determination of $\mathcal{A}$ from the scattering matrix $\mathcal{S}$ requires that all of the complex elements of $\mathcal{S}$ are known, while the measurement of the exit-surface wave function for a single orientation provides (*via* a Fourier transform) only elements of one column of $\mathcal{S}$ (Allen *et al.*, 1999). The elements in the other columns of the $\mathcal{S}$ matrix can be found by transforming the exit-surface wave function obtained at well defined secondary orientations. These secondary orientations are related to the principal orientation by changes in the components of the incident wavevector by a reciprocal-lattice vector, all of which are assumed to be confined to the zero-order Laue zone (Allen *et al.*, 1998, 1999; Spence, 1998). The phase-retrieval techniques discussed in the previous paragraph can, in principle, also be used at these secondary orientations to determine the exit-surface wave function.

A solution to the problem of retrieving the structure matrix $\mathcal{A}$ from the scattering matrix $\mathcal{S}$ in dynamical electron diffraction (at a fixed energy) has recently been given (Allen *et al.*, 1999). Absorption of electrons from the elastically scattered beams is not catered for in that work but, for thicker crystals, absorption is a crucial part of the physics. The inverse scattering method proceeds *via* sets of linear equations which allow a unique determination of $\mathcal{A}$. Constraints are provided by the fact that the diagonal elements of $\mathcal{A}$ are known (determined by the principal orientation of the incident beam) and that $\mathcal{A}$ has general symmetries across its antidiagonal. For a symmetric orientation of the incident beam, the symmetries across the antidiagonal of $\mathcal{A}$ yield trivial constraints and the orientation information in the diagonal of $\mathcal{A}$ is insufficient to determine $\mathcal{A}$ from $\mathcal{S}$ uniquely. However, it is experimentally convenient to work at this orientation. Furthermore, correct phasing of the $\mathcal{S}$ matrix is facilitated by the fact that, for a symmetric orientation, it has (nontrivial) symmetries across its antidiagonal similar to those in $\mathcal{A}$ (Spence, 1998; Allen *et al.*, 1998, 1999). In this paper, inversion of the dynamical scattering including absorption and for any principal orientation of the incident beam is addressed. The projected potentials associated with both the elastic and the absorptive scattering can be uniquely obtained from the scattering matrix $\mathcal{S}$.

The inversion of dynamical electron diffraction is also being addressed from other perspectives. Examples of very recent work are that due to Spence *et al.* (1999), who have discussed a method limited to centrosymmetric structures based on projection onto convex sets, Rez (1999), who has suggested schemes to determine the crystal potential by varying the incident energy, and Sinkler & Marks (1999), who have discussed the use of minimum-relative-entropy approaches.

2. The forward-scattering problem

In this section, we give the essential points of the forward (direct) problem for the scattering of high-energy electrons, taking into account absorptive scattering. The Schrödinger equation can be cast in the form of an eigenvalue problem (Humphreys, 1979; Allen & Rossouw, 1989):

$$\mathcal{A}\mathcal{C} = \mathcal{C}[2K\lambda^i]_D. \tag{1}$$

Here $\mathcal{A}$ is the structure (Bethe) matrix and has the form

$$\mathcal{A} = \begin{pmatrix} & \vdots & \vdots & \vdots & \vdots & \vdots & \\ \cdots & -(\mathbf{k}_t+\mathbf{h})^2 + iU'_{\mathbf{0}} & W_{\mathbf{h}-\mathbf{g}} & W_{\mathbf{h}} & W_{\mathbf{h}+\mathbf{g}} & W_{2\mathbf{h}} & \cdots \\ \cdots & W_{\mathbf{g}-\mathbf{h}} & -(\mathbf{k}_t+\mathbf{g})^2 + iU'_{\mathbf{0}} & W_{\mathbf{g}} & W_{2\mathbf{g}} & W_{\mathbf{g}+\mathbf{h}} & \cdots \\ \cdots & W_{-\mathbf{h}} & W_{-\mathbf{g}} & -\mathbf{k}_t^2 + iU'_{\mathbf{0}} & W_{\mathbf{g}} & W_{\mathbf{h}} & \cdots \\ \cdots & W_{-\mathbf{g}-\mathbf{h}} & W_{-2\mathbf{g}} & W_{-\mathbf{g}} & -(\mathbf{k}_t-\mathbf{g})^2 + iU'_{\mathbf{0}} & W_{-\mathbf{g}+\mathbf{h}} & \cdots \\ \cdots & W_{-2\mathbf{h}} & W_{-\mathbf{h}-\mathbf{g}} & W_{-\mathbf{h}} & W_{-\mathbf{h}+\mathbf{g}} & -(\mathbf{k}_t-\mathbf{h})^2 + iU'_{\mathbf{0}} & \cdots \\ & \vdots & \vdots & \vdots & \vdots & \vdots & \end{pmatrix}, \tag{2}$$

where $\mathbf{g}$ and $\mathbf{h}$ are reciprocal-lattice vectors and

$$W_{\mathbf{g}} = U_{\mathbf{g}} + iU'_{\mathbf{g}}. \tag{3}$$

The $W_{\mathbf{g}}$ are Fourier coefficients in the optical potential for the scattering of electrons from the crystal. The real part of the periodic crystal potential (associated mainly with elastic Coulomb scattering) is written as

$$V(\mathbf{r}) = (\hbar^2/2m)\sum_{\mathbf{g}} U_{\mathbf{g}} \exp(i\mathbf{g}\cdot\mathbf{r}). \tag{4}$$

The effect of absorptive (inelastic) scattering processes is taken into account by a component $iV'(\mathbf{r})$ in the optical potential and $V'(\mathbf{r})$ is written as

$$V'(\mathbf{r}) = (\hbar^2/2m)\sum_{\mathbf{g}} U'_{\mathbf{g}} \exp(i\mathbf{g}\cdot\mathbf{r}). \tag{5}$$

The wavevector $\mathbf{k}_t$ in equation (2) is the tangential component of the incident electron wavevector $\mathbf{k}$ in vacuum, along the plane defined by the reciprocal-lattice vectors. K is the magnitude of the incoming wavevector corrected for refraction, *i.e.* $K^2 = k^2 + U_{\mathbf{0}}$, where $U_{\mathbf{0}}$ gives the mean of the crystal potential associated with elastic scattering. The matrix $\mathcal{C}$ has as columns the eigenvectors of $\mathcal{A}$ and can be explicitly written as follows:

$$\mathcal{C} = \begin{pmatrix} \vdots & \vdots & \vdots & \vdots & \\ C^1_{\mathbf{h}} & C^2_{\mathbf{h}} & \cdots & C^i_{\mathbf{h}} & \cdots \\ C^1_{\mathbf{g}} & C^2_{\mathbf{g}} & \cdots & C^i_{\mathbf{g}} & \cdots \\ C^1_{\mathbf{0}} & C^2_{\mathbf{0}} & \cdots & C^i_{\mathbf{0}} & \cdots \\ C^1_{-\mathbf{g}} & C^2_{-\mathbf{g}} & \cdots & C^i_{-\mathbf{g}} & \cdots \\ C^1_{-\mathbf{h}} & C^2_{-\mathbf{h}} & \cdots & C^i_{-\mathbf{h}} & \cdots \\ \vdots & \vdots & \vdots & \vdots & \end{pmatrix}. \tag{6}$$

Lastly, in equation (1), $[2K\lambda^i]_D$ is the diagonal matrix containing the (complex) eigenvalues of $\mathcal{A}$.

Since the potentials $V(\mathbf{r})$ and $V'(\mathbf{r})$ given by equations (4) and (5), respectively, are real, $U_{\mathbf{g}} = U^*_{-\mathbf{g}}$ and $U'_{\mathbf{g}} = U'^*_{-\mathbf{g}}$. (We make the assumption that, for every reciprocal-lattice vector $\mathbf{g}$, the vector $-\mathbf{g}$ is included in the representation of $\mathcal{A}$.) However, in the presence of absorption, $(U_{\mathbf{g}} + iU'_{\mathbf{g}}) \neq (U_{-\mathbf{g}} + iU'_{-\mathbf{g}})^*$ and $\mathcal{A}$ is not hermitian. Thus, the matrix of eigenvectors given by equation (6) is not unitary.

Let us assume an N-beam approximation ($\mathcal{A}$ becomes an $N \times N$ matrix). Furthermore, let us relabel the elements of the corresponding $N \times N$ eigenvector matrix $\mathcal{C}$ as follows:

$$\mathcal{C} = \begin{pmatrix} C_{11} & C_{12} & \cdots & C_{1i} & \cdots & C_{1N} \\ C_{21} & C_{22} & \cdots & C_{2i} & \cdots & C_{2N} \\ \vdots & \vdots & \vdots & \vdots & \vdots & \vdots \\ C_{N1} & C_{N2} & \cdots & C_{Ni} & \cdots & C_{NN} \end{pmatrix}. \tag{7}$$

This relabelling facilitates writing down the representation for the elements of $\mathcal{A}$, which follows from equation (1). Let the reciprocal-lattice vector $\mathbf{g}_n$ occur in the nth row of equation (7) and similarly for $\mathbf{g}_m$. Then we can write

$$\mathcal{A}_{\mathbf{g}_n,\mathbf{g}_m} = 2K\sum_i C_{ni}\lambda^i [C^{-1}]_{im}, \tag{8}$$

where the sum extends over N terms. $[C^{-1}]_{im}$ is the element in the ith row and mth column of the inverse of $\mathcal{C}$. The change in notation for the elements of $\mathcal{C}$ will also facilitate writing down some later equations.

The elements of the matrix $\mathcal{C}$ and the eigenvalues $2K\lambda^i$ allow us to construct the wave function of the fast electron in the crystal as a sum of Bloch states,

$$\psi(\mathbf{r}) = \sum_i \alpha^i \varphi^i(\mathbf{r}) = \sum_i \alpha^i \sum_{\mathbf{g}} C^i_{\mathbf{g}} \exp[i(\mathbf{k}^i + \mathbf{g})\cdot\mathbf{r}]. \tag{9}$$

Each Bloch state $\varphi^i(\mathbf{r})$ is characterized by an intrinsic wavevector $\mathbf{k}^i$ which depends on the energy of the incident beam as well as on the crystal structure and can be obtained from the

solution of the Schrödinger equation. The wavevectors $\mathbf{k}^i$ can be expressed in the form $\mathbf{k}^i = \mathbf{K} + \lambda^i \hat{\mathbf{n}}$, where $\mathbf{K}$ is the wavevector of the incoming plane wave in the crystal and the complex eigenvalue $\lambda^i = \gamma^i + i\eta^i$ (Humphreys, 1979; Allen & Rossouw, 1989). The unit vector $\hat{\mathbf{n}}$ is a surface normal directed into the entrance crystal surface, the γ^i are the *Anpassung* and the η^i the absorption coefficients. The α^i are obtained from the boundary conditions at the entrance surface of the crystal, which require that the amplitude of the directly transmitted beam is 1 and the amplitudes of the diffracted beams are 0. It is found (Sheinin & Jap, 1979; Allen & Rossouw, 1989) that $\alpha^i = [C^{-1}]_{i,(N+1)/2}$, *i.e.* it is the ith element in the central column of C^{-1}. At the exit surface of the crystal, the Bloch waves decouple into plane waves. At this transition, the tangential components remain unchanged and therefore the amplitude of the beam $\mathbf{g}$ for a crystal of thickness t is obtained from equation (8) as

$$v_{\mathbf{g}}(t) = \sum_i \alpha^i C^i_{\mathbf{g}} \exp(i\lambda^i t). \tag{10}$$

Introducing the vector $\mathbf{v} = (v_{\mathbf{g}})$, we can write equation (8) in the compact form

$$\mathbf{v} = \mathcal{S}\mathbf{u}. \tag{11}$$

The vector $\mathbf{u} = (\delta_{\mathbf{g0}})$ characterizes the incident beam (a plane wave) and

$$\mathcal{S} = \exp[(it/2K)\mathcal{A}] = \mathcal{C}[\exp(i\lambda^i t)]_D \mathcal{C}^{-1} \equiv \mathcal{C}[\Lambda^i]_D \mathcal{C}^{-1} \tag{12}$$

is the scattering matrix, where once again $[\,]_D$ denotes a diagonal matrix. The scattering matrix relates the incident electron wave at the entrance surface of the crystal to the diffracted wave at the exit surface of the crystal of thickness t (Humphreys, 1979). Note that, since $\mathcal{A}$ is not hermitian when absorption is included, $\mathcal{S}$ is not unitary. Schematically, we can represent $\mathcal{S}$ as

$$\mathcal{S} = \begin{pmatrix} & \vdots & \vdots & \vdots & \vdots & \vdots & \\ \cdots & S_{\mathbf{h},\mathbf{h}} & S_{\mathbf{h},\mathbf{g}} & S_{\mathbf{h},\mathbf{0}} & S_{\mathbf{h},-\mathbf{g}} & S_{\mathbf{h},-\mathbf{h}} & \cdots \\ \cdots & S_{\mathbf{g},\mathbf{h}} & S_{\mathbf{g},\mathbf{g}} & S_{\mathbf{g},\mathbf{0}} & S_{\mathbf{g},-\mathbf{g}} & S_{\mathbf{g},-\mathbf{h}} & \cdots \\ \cdots & S_{\mathbf{0},\mathbf{h}} & S_{\mathbf{0},\mathbf{g}} & S_{\mathbf{0},\mathbf{0}} & S_{\mathbf{0},-\mathbf{g}} & S_{\mathbf{0},-\mathbf{h}} & \cdots \\ \cdots & S_{-\mathbf{g},\mathbf{h}} & S_{-\mathbf{g},\mathbf{g}} & S_{-\mathbf{g},\mathbf{0}} & S_{-\mathbf{g},-\mathbf{g}} & S_{-\mathbf{g},-\mathbf{h}} & \cdots \\ \cdots & S_{-\mathbf{h},\mathbf{h}} & S_{-\mathbf{h},\mathbf{g}} & S_{-\mathbf{h},\mathbf{0}} & S_{-\mathbf{h},-\mathbf{g}} & S_{-\mathbf{h},-\mathbf{h}} & \cdots \\ & \vdots & \vdots & \vdots & \vdots & \vdots & \end{pmatrix}. \tag{13}$$

Let the reciprocal-lattice vector $\mathbf{g}_n$ correspond to the nth row of equation (7) and similarly for $\mathbf{g}_m$. Then, for an N-beam approximation, we have the representation

$$\mathcal{S}_{\mathbf{g}_n,\mathbf{g}_m} = \sum_i C_{ni} \exp(i\lambda^i t)[C^{-1}]_{im} \tag{14}$$

for the $\mathcal{S}$ matrix.

3. The inverse scattering problem

The inverse scattering problem is to obtain $\mathcal{A}$ from a knowledge of $\mathcal{S}$, which we assume has been fully determined, as discussed in the *Introduction*. From equation (12), we can write

$$\mathcal{A} = (2K/it)\ln(\mathcal{S}) = (2K/it)\mathcal{C}\ln[\Lambda^i]_D\mathcal{C}^{-1} = (2K/it)\mathcal{C}[i\lambda^i t]_D\mathcal{C}^{-1}. \tag{15}$$

This expresses $\mathcal{A}$ in terms of the eigenvectors and eigenvalues of $\mathcal{S}$. [It can easily be shown from equation (12) that the eigenvectors of $\mathcal{S}$ are the same as those of $\mathcal{A}$.] However, in taking the natural logarithm of $[\Lambda^i]_D$ (which, since it is a diagonal matrix, means taking the natural logarithm of each diagonal element), ambiguities arise since

$$\ln(\Lambda^i) = i\lambda^i t = \ln|\Lambda^i| + i(\theta^i + 2n^i\pi), \quad n^i = 0, \pm1, \pm2, \ldots, \tag{16}$$

where θ^i is the principal value of the amplitude of Λ^i. The logarithm is an infinitely many valued function.

To resolve these ambiguities, we proceed in a manner analogous to that outlined by Allen *et al.* (1999) for the case of elastic scattering only, except that here we will also provide a solution for symmetric orientations of the incident beam. With the inclusion of absorption, the elements on the diagonal of the $\mathcal{A}$ matrix are given by $\mathcal{A}_{\mathbf{g}_n,\mathbf{g}_n} = -(\mathbf{k}_t + \mathbf{g}_n)^2 + iU'_{\mathbf{0}}$, where the additional term $U'_{\mathbf{0}}$ gives the mean value of the absorption potential. This leads to a set of N linear equations in the N unknown λ^i's:

$$\sum_i C_{ni}[C^{-1}]_{in}\lambda^i = [-(\mathbf{k}_t + \mathbf{g}_n)^2 + iU'_{\mathbf{0}}]/2K, \tag{17}$$

where the matrix elements C_{ni} and $[C^{-1}]_{in}$ are obtained after diagonalizing $\mathcal{S}$. The use of these equations in the dynamical inversion implies an *a priori* knowledge of both $U_{\mathbf{0}}$ and $U'_{\mathbf{0}}$ (the former implicit in K). If $U_{\mathbf{0}}$ is not known, the approximation $K \approx k$ is a good one for high-energy electrons. We could also simply neglect the term $U'_{\mathbf{0}}$. We will investigate these approximations in our model calculations in the next section.

Further linear equations involving the λ^i's can be obtained using the fact that $\mathcal{A}_{\mathbf{g}_k,\mathbf{g}_l} = U_{\mathbf{g}_k-\mathbf{g}_l} = U_{\mathbf{g}_m-\mathbf{g}_n} = \mathcal{A}_{\mathbf{g}_m,\mathbf{g}_n}$ whenever $\mathbf{g}_k - \mathbf{g}_l = \mathbf{g}_m - \mathbf{g}_n$, for $k \neq l$ and $m \neq n$. Using equation (8), these symmetries lead to the following set of homogeneous linear equations:

$$\sum_i (C_{ki}[C^{-1}]_{il} - C_{mi}[C^{-1}]_{in})\lambda^i = 0$$
$$\text{whenever} \quad \mathbf{g}_k - \mathbf{g}_l = \mathbf{g}_m - \mathbf{g}_n, \quad \text{for} \quad k \neq l \quad \text{and} \quad m \neq n. \tag{18}$$

Here, $\mathbf{g}_j$ refers to the reciprocal-lattice vector defining the jth row of $\mathcal{C}$ given in equation (7). A subset of these equations, which are always present in the $\mathcal{A}$ matrix, are symmetries that $\mathcal{A}$ has across its antidiagonal (Allen *et al.*, 1998, 1999) given by $\mathcal{A}_{k,l} = \mathcal{A}_{N+1-l,N+1-k}$, with $k \neq l$ if $\mathbf{k}_t \neq 0$ and where k and l label rows and columns in $\mathcal{A}$, respectively. Using equation (4), we can express this as follows:

$$\sum_i (C_{ki}[C^{-1}]_{il} - C_{N+1-l,i}[C^{-1}]_{i,N+1-k})\lambda^i = 0$$
$$\text{with} \quad k \neq l \quad \text{if} \quad \mathbf{k}_t \neq 0 \quad \text{and} \quad k + l \leq N. \tag{19}$$

The remaining constraints of the type given by (18) and independent of those given by (19) are found by confining ourselves to the antidiagonal of $\mathcal{A}$ and above to give

$$\sum_i (C_{ki}[C^{-1}]_{il} - C_{mi}[C^{-1}]_{in})\lambda^i = 0 \quad \text{with} \quad \mathbf{g}_k - \mathbf{g}_l = \mathbf{g}_m - \mathbf{g}_n,$$
$$k + l \leq N + 1 \quad \text{and} \quad m + n \leq N + 1. \tag{20}$$

Fig. 1 shows the indexing of the $\mathcal{A}$ matrix for the [110] zone axis in a face-centered-cubic system (such as GaAs) in a seven-beam approximation. The central column shows the pertinent seven reciprocal-lattice vectors. The symmetries across the antidiagonal evident in equation (2) and leading to equation (19) are explicitly seen in Fig. 1 for this case – for example, one of these symmetries (there are 18 in total) is indicated by the two ringed indices that each have the value $(1, \bar{1}, 3)$. There are six symmetries leading to constraints of the type given by equations (20), as indicated. We will investigate the use of these relations in uniquely retrieving the eigenvalues $2K\lambda^i$ of $\mathcal{A}$ in the next section. For a zone-axis case, the symmetries given by equations (20) are obtained by inspection of the indexing of the $\mathcal{A}$ matrix for the particular space group considered. However, for a systematic row orientation, we observe that the $\mathcal{A}$ matrix becomes a band matrix of the form

$$\mathcal{A} = \begin{pmatrix}
 & \vdots & \vdots & \vdots & \vdots & \vdots & \\
\cdots & -(\mathbf{k}_t + 2\mathbf{g})^2 + iU_0' & W_{\mathbf{g}} & W_{2\mathbf{g}} & W_{3\mathbf{g}} & W_{4\mathbf{g}} & \cdots \\
\cdots & W_{-\mathbf{g}} & -(\mathbf{k}_t + \mathbf{g})^2 + iU_0' & W_{\mathbf{g}} & W_{2\mathbf{g}} & W_{3\mathbf{g}} & \cdots \\
\cdots & W_{-2\mathbf{g}} & W_{-\mathbf{g}} & -\mathbf{k}_t^2 + iU_0' & W_{\mathbf{g}} & W_{2\mathbf{g}} & \cdots \\
\cdots & W_{-3\mathbf{g}} & W_{-2\mathbf{g}} & W_{-\mathbf{g}} & -(\mathbf{k}_t - \mathbf{g})^2 + iU_0' & \cdots & \\
\cdots & W_{-4\mathbf{g}} & W_{-3\mathbf{g}} & W_{-2\mathbf{g}} & W_{-\mathbf{g}} & -(\mathbf{k}_t - 2\mathbf{g})^2 + iU_0' & \cdots \\
 & \vdots & \vdots & \vdots & \vdots & \vdots &
\end{pmatrix}. \tag{21}$$

This means the symmetries given by equation (20) are *generally* evident, owing to the band structure of $\mathcal{A}$ which occurs irrespective of the space group or systematic row.

If $\mathbf{k}_t = \mathbf{0}$, then equations (19) also hold for $k = l$. Thus, we have a matrix for which the given symmetry is true for *all* elements on or above the anti-diagonal. The coefficients of λ^i in equation (19) are then all zero (see Appendix *A*). When $\mathbf{k}_t = \mathbf{0}$, equations (17) are no longer linearly independent and yield at most $(N + 1)/2$ linearly independent (complex) equations, while we must find N complex parameters λ^i. This is similar to the case of no absorption (Allen *et al.*, 1999). We then must use equations (17) and (20) to uniquely obtain the λ^i and hence $\mathcal{A}$. N needs to be large enough for equations (17) and (20) to have a coefficient matrix that is rank N (it is evident that $N = 3$ will not work). However, this is not an important restriction in practice, as we will see in the next section. Furthermore, the rank of the set of linear equations we use to obtain the λ^i, and thus the uniqueness of the solution, is easily checked and there is no danger of unwittingly obtaining a spurious solution to the inversion problem.

Having solved the inversion step $\mathcal{S} \rightarrow \mathcal{A}$, we can calculate the Fourier coefficients $U_{\mathbf{g}}$ and $U_{\mathbf{g}}'$ in equations (4) and (5) from (Spence, 1993)

$$U_{\mathbf{g}} = (W_{\mathbf{g}} + W_{-\mathbf{g}}^*)/2 \quad \text{and} \quad U_{\mathbf{g}}' = (W_{\mathbf{g}} - W_{-\mathbf{g}}^*)/2i. \tag{22}$$

The potential associated with elastic scattering and that due to absorption can thus each be recovered separately.

4. Model solutions of the inverse scattering problem

We consider the [110] zone axis in GaAs as an example and calculate the $\mathcal{S}$ matrix, which is then used as input in testing our inversion procedure. Our calculations were for an incident electron energy of 400 keV and a crystalline slab of thickness 1000 Å. However, the method works for arbitrary incident energy and sample thickness. The thickness need not be known explicitly. We will continue with $N = 7$ for our detailed example, chosen for simplicity of illustration, but we emphasize that the method works just as well for larger values of N. The Fourier coefficients for the elastic potential were calculated using the electron scattering factors provided by Waasmaier & Kirfel (1995) and thermal effects are incorporated *via* a Debye–Waller factor. A temperature factor $B = 0.6$ Å^2 was used for both Ga and As, as was done by Lentzen & Urban (1996) and subsequently by Allen *et al.* (1998). Absorption will

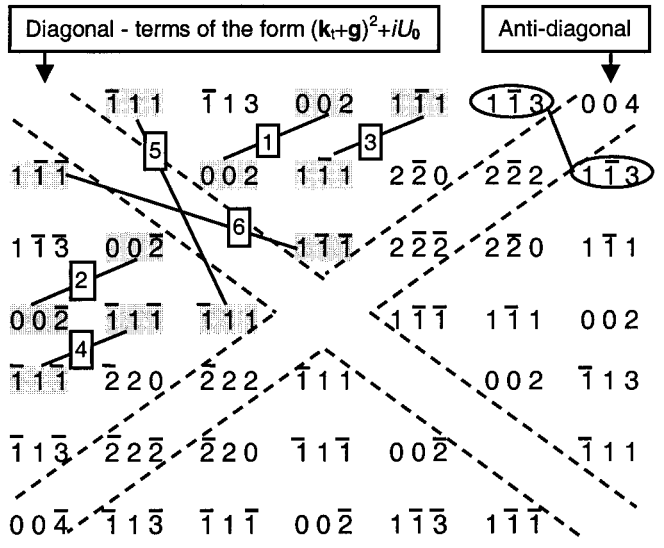

Figure 1
Indexing of the structure matrix for the [110] zone axis for a face-centered-cubic structure. A symmetry of the type given by equation (19) is indicated by the ringed elements, each labelled $1\bar{1}3$. Six symmetries of the type given by equation (20) are evident above the antidiagonal.

be included in the calculations assuming that it is due to thermal diffuse scattering (TDS) based on an Einstein model (Hall & Hirsch, 1965; Allen & Rossouw, 1989; Bird & King, 1990). TDS is the main absorptive mechanism leading to loss of diffraction contrast. The real part of the projected potential $V(\mathbf{r})$ is shown in Fig. 2(*a*) and the potential $V'(\mathbf{r})$ representing absorption due to TDS is shown in Fig. 2(*b*). These representations of the potential (each with 19 Fourier coefficients) are of course not converged, as can be seen by comparison with Fig. 1 in Allen & Rossouw (1993), where many more Fourier coefficients were used to plot the potentials. It is worth noting that, while $V(\mathbf{r})$ is intrinsic to the crystal, depending only on the temperature, $V'(\mathbf{r})$ (for TDS) is energy-dependent.

The $\mathcal{S}$ matrix has been calculated and then diagonalized to find its eigenvectors for each of the principal orientations shown in Table 1. The outcomes of retrieving the set $\{\lambda^i\}$ correctly (uniquely) using equations (17) alone, equations (17) and (19), and then equations (17) and (20) to determine the parameters $\{\lambda^i\}$ are noted. We solve the set of linear equations to obtain the $\{\lambda^i\}$ using the method of singular-value decomposition (SVD) as discussed by Press *et al.* (1992), which easily accommodates the solution of more equations than unknowns. As expected, there is insufficient information to determine the λ^i in the symmetric orientation using equations (17) and (19). We must then use equations (17) and (20). For the [110] zone in a face-centered-cubic structure, equations (20) arise from the symmetries labelled 1 to 6 in Fig. 1. For $\mathbf{k}_t = (000)$, equations (17) yield only three linearly independent equations for the λ^i out of $(N+1)/2 = 4$ possible linearly independent equations, since the equations relating to the {110}-type reflections are the same. The symmetries labelled 1 to 4 in Fig. 1 yield the remaining four equations that are required to determine the λ^i uniquely. It should be noted that the symmetries labelled by 5 and 6 yield similar equations to those

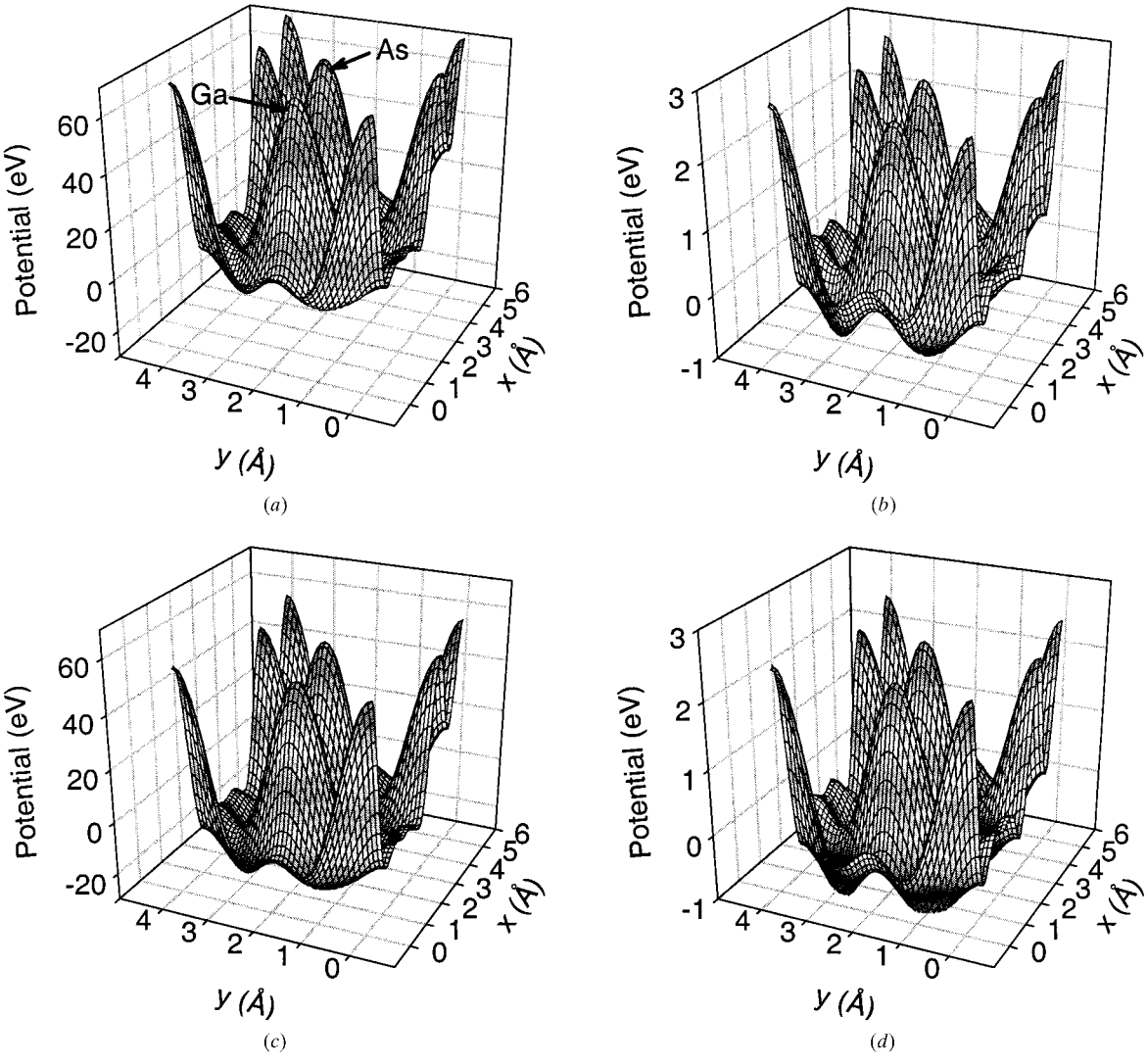

Figure 2
Real and imaginary (absorptive) parts of the optical potential for the [110] zone axis in GaAs. (*a*) The input model real potential (mean potential V_0 included). (*b*) The input absorptive potential (mean potential V'_0 included). The potentials obtained by inversion, assuming that V_0 and V'_0 are known, are the same as those in (*a*) and (*b*) to high accuracy and indistinguishable on the scale of the figure. Assuming that V'_0 and V_0 are not known for the purposes of inversion and assumed zero, we obtain the real potential and absorptive potential shown in (*c*) and (*d*), respectively.

Table 1
The $\mathcal{S}$ matrix has been calculated for each of the indicated principal orientations about the [110] zone axis in GaAs (incident energy 400 keV, thickness 1000 Å, including absorption in the form of TDS and using $N = 7$ beams).

The outcomes of retrieving the complex eigenvalues $2K\lambda^i$ of the structure matrix $\mathcal{A}$ uniquely using equations (17), equations (17) and (19), and then equations (17) and (20) are noted.

Case	$\mathbf{k}_t$	Equation (17)	Equations (17)+(19)	Equations (17)+(20)
1	$(0, 0, 0)$	No	No	Yes
2	$(0, 0, \bar{1})$	No	Yes	Yes
3	$(\bar{1}, 1, 0)$	No	Yes	Yes
4	$(\bar{\frac{1}{2}}, \frac{1}{2}, \bar{\frac{1}{2}})$	Yes	Yes	Yes
5	$(1, \bar{1}, \frac{3}{4})$	Yes	Yes	Yes

labelled by 3 and 4, respectively. It is also worth pointing out that while the equations obtained from symmetries 1 and 2 are complex conjugates, complex conjugation is not a linear operation and thus the equations are linearly independent. When $\mathbf{k}_t = (00\bar{1})$, *i.e.* the reflection 002 is in the exact Bragg orientation (case 2), then there is still sufficient symmetry in the system to render equations (17) linearly dependent. However, addition of the symmetry constraints, equations (19), determines the $\{\lambda^i\}$ uniquely. Tilting along the $[\bar{1}10]$ direction gives similar results. Tilting so that the reflection $1\bar{1}1$ is in the exact Bragg orientation removes symmetries and allows a unique determination of the $\{\lambda^i\}$ *via* equations (17). A similar breaking of symmetries occurs for the arbitrary orientation given in case 5 and once again the orientation constraints are sufficient to solve for the $\{\lambda^i\}$. We have assumed that the mean potentials are known in these tests. With this assumption, the potentials shown in Figs. 2(*a*) and 2(*b*) are retrieved to high precision (at least six-figure accuracy). The results are not significantly changed if we assume that $K \approx k$ since, at 400 keV, $K = 60.8326$ Å^{-1} and $k = 60.8311$ Å^{-1}. Assuming both $V_{\mathbf{0}} = 0$ and $V'_{\mathbf{0}} = 0$, we obtain by inversion the potentials shown in Figs. 2(*c*) and 2(*d*). The real and absorptive potentials obtained from the exact and approximate inversions differ by the mean potentials $V_{\mathbf{0}} = 14.68$ and $V'_{\mathbf{0}} = 0.3164$ eV, respectively. The differences are exact to the number of figures quoted for the mean potentials. This is consistent with the level of agreement between K and k. It is not surprising that the approximate inversion only amounts to these shifts, since $V'(\mathbf{r})$ is an order of magnitude smaller than $V(\mathbf{r})$ and the absorptive scattering can be treated perturbatively (Humphreys, 1979; Allen & Rossouw, 1989).

Next we have tested the use of equations (17) and (20) to solve the dynamical inversion problem for $\mathbf{k}_t = \mathbf{0}$ for several crystals, systematic rows and zone axes. Provided that the number of beams is large enough (typically of the order of ten), then a unique reconstruction of $\mathcal{A}$ from $\mathcal{S}$ was always achieved. [We note that, in contrast, when using equations (17) and (19) for $\mathbf{k}_t \neq \mathbf{0}$, unique solutions to the inverse scattering problem can be found for any odd $N \geq 3$.] These results are shown in Table 2. The results found are independent of incident energy and crystal temperature and thickness. For all the results shown, with the exception of those in the last line, the number of beams indicated is the minimum number for which the inversion procedure worked, and not excluding any beams with the same magnitude (scattering angle) as those already in the set. For example, for the [111] zone axis in GaAs or Si, 15 beams are sufficient but this excludes some reciprocal-lattice vectors of the same magnitude as some already included. All systematic row cases required only five beams. Notice that, for the [110] zone-axis case in Si, which is centrosymmetric, nine beams were required for a unique solution, unlike GaAs (noncentrosymmetric), which required only seven. The centrosymmetry of silicon means that the origin of the unit cell can be chosen so that the structure factors are real. Then the equations that are obtained from symmetries 1 and 2, which are related by complex conjugation, become identical. In practice, it is likely that a unique solution to the inversion problem for the symmetric orientation using equations (17) and (20) will be possible for values of N well below those giving a reasonable representation of the dynamical scattering. The increase in the number of symmetries, leading to constraints of the type in equations (20), with N is shown in Fig. 3 for the [110] zone axis in a face-centered-cubic structure. The results in the last line of Table 2, for GaAs with 129 beams and the superconductor $Bi_2Sr_2CaCu_2O_8$ with 67 beams, show that the inversion method works for large numbers of beams and for more complex structures.

Table 2
Test cases for several crystals for a number of exact symmetric (systematic row) or zone-axis orientations which provide a unique solution to the dynamical inversion problem using equations (17) and (20).

Crystal	Systematic row/zone axis	N
GaAs	[110] zone axis	7
GaAs	[100] zone axis	13
GaAs	[111] zone axis	19
GaAs	[332] zone axis	7
GaAs	{100} systematic row	5
GaAs	{111} systematic row	5
GaAs	[110] zone axis	129
Si	[110] zone axis	9
Si	[100] zone axis	13
Si	[111] zone axis	19
Si	[332] zone axis	7
Si	{100} systematic row	5
Si	{111} systematic row	5
$Bi_2Sr_2CaCu_2O_8$	[001] zone axis	67

Lastly, we note that degeneracies in the eigenvalues of $\mathcal{S}$ (and hence those of $\mathcal{A}$) do not pose a problem for the inversion method. For example, consider the second case in Table 2, namely the GaAs [100] zone axis with $N = 13$. In that case, there are three degenerate eigenvalues.

5. Summary and conclusions

The main steps in the inversion of the dynamical scattering, taking into account absorptive processes, can be described as follows. We assume that all the complex elements of the

scattering matrix $\mathcal{S}$, for a given energy and thickness, have been determined (up to an arbitrary overall phase) using a through-tilt series of measurements at the principal and well defined secondary orientations of the incident beam. $\mathcal{S}$ is then diagonalized to obtain its eigenvectors. The eigenvectors of $\mathcal{S}$ and $\mathcal{A}$ are the same. The eigenvalues $2K\lambda^i$ of $\mathcal{A}$ are then obtained uniquely using equations (17) (following from knowledge about the diagonals of $\mathcal{A}$, which are determined by the principal orientation, $U_{\mathbf{0}}$ and $U'_{\mathbf{0}}$) and (19) (derived from general symmetries of $\mathcal{A}$ across its antidiagonal) or (20). For an exact zone-axis orientation of the incident beam, when we must use equations (20), N needs to be large enough. However, this is a constraint which is likely to be always satisfied when realistically modeling the dynamical scattering with a sufficient number of beams. The matrix $\mathcal{A}$ is then constructed (uniquely) from its eigenvectors and eigenvalues using the representation of $\mathcal{A}$ given by (8). Both the projected potential associated with elastic scattering and that associated with absorption are obtained. Note that it is not necessary to know the thickness of the crystalline slab explicitly.

The inversion of the dynamical scattering proceeds *via* the solution of sets of linear equations, yields a unique solution and is numerically stable. The main challenge in the practical implementation of the methods discussed here is the accurate determination of the scattering matrix $\mathcal{S}$. The amplitude and phase of all elements needs to be known. This requires the determination of the exit-surface wave function at the principal and secondary orientations of the incident beam. Work on phase retrieval to date, of which we are aware, has been limited to the symmetric orientation of the incident beam. Methods using conservation of flux (Van Dyck & Coene, 1987) are likely to need modification for significant tilts away from the symmetric orientation. Furthermore, in the determination of $\mathcal{S}$, errors in orientation and energy of the incident beam, lens aberrations, detector noise *etc.* will need to be carefully considered. Lens apertures restrict the number of beams contributing to images and the number of beams that are important may vary with thickness. These issues will be investigated in future work.

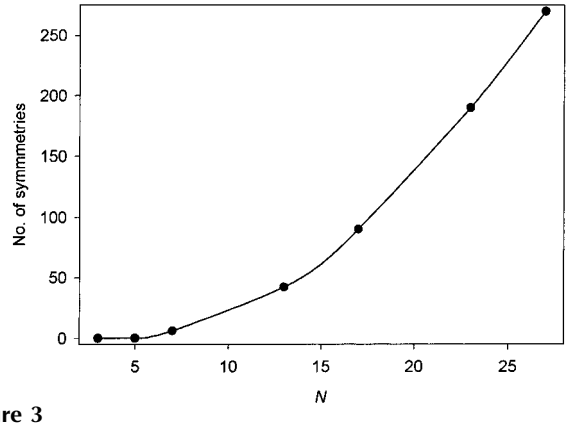

Figure 3
Number of symmetries leading to equations of the type (20) as a function of N (the dimension of the structure matrix $\mathcal{A}$) for the [110] zone axis in a face-centered-cubic structure.

APPENDIX *A*

From equation (1), we can express the eigenvalues of $\mathcal{A}$ as

$$2K\lambda^i = \sum_k \sum_l [C^{-1}]_{ik} A_{kl} C_{li}. \tag{23}$$

Assume that $\mathbf{k}_t = \mathbf{0}$. Then $\mathcal{A}_{k,l} = \mathcal{A}_{N+1-l,N+1-k}$ for all k and l. It then follows that $\mathcal{A}^t_{k,l} = \mathcal{A}_{N+1-k,N+1-l}$, where t denotes an element in the transpose. Now, using the fact that $[2K\lambda^i]_D$ is a diagonal matrix, and therefore is its own transpose, we can write

$$\begin{aligned} 2K\lambda^i &= \sum_k \sum_l [C]^t_{ik} A^t_{kl} [C^{-1}]^t_{li} \\ &= \sum_k \sum_l [C]_{ki} A_{N+1-k,N+1-l} [C^{-1}]_{il}. \end{aligned} \tag{24}$$

Now, making the change of variables $m = N + 1 - k$ and $n = N + 1 - l$, we obtain

$$2K\lambda^i = \sum_m \sum_n C_{N+1-m,i} A_{mn} [C_{-1}]_{i,N+1-n}. \tag{25}$$

From equations (23) and (25), it follows that

$$\sum_k \sum_l (C_{ki}[C^{-1}]_{il} - C_{N+1-l,i}[C^{-1}]_{i,N+1-k}) A_{lk} = 0. \tag{26}$$

This can only be true for *any* choice of the matrix elements A_{lk} if their coefficients are all zero.

LJA acknowledges financial support from the Australian Research Council. LJA appreciates the warm hospitality extended to him during a visit to the Technische Universität Wien and thanks Dr Mark Oxley and Dr Alan Spargo for helpful discussions.

References

Allen, L. J., Josefsson, T. W. & Leeb, H. (1998). *Acta Cryst.* A**54**, 388–398.
Allen, L. J., Leeb, H. & Spargo, A. E. C. (1999). *Acta Cryst.* A**55**, 105–111.
Allen, L. J. & Rossouw, C. J. (1989). *Phys. Rev. B*, **39**, 8313–8321.
Allen, L. J. & Rossouw, C. J. (1993). *Phys. Rev. B*, **47**, 2446–2452.
Beeching, M. J. & Spargo, A. E. C. (1993). *Ultramicroscopy*, **52**, 243–247.
Bird, D. M. & King, Q. A. (1990). *Acta Cryst.* A**46**, 202–208.
Coene, W., Janssen, G., Op de Beeck, M. & Van Dyck, D. (1992). *Phys. Rev. Lett.* **69**, 3743–3746.
Dorset, D. L. (1995). *Acta Cryst.* A**51**, 869–879.
Gilmore, C. J. (1996). *Acta Cryst.* A**52**, 561–589.
Gribelyuk, M. A. (1991). *Acta Cryst.* A**47**, 715–723.
Gribelyuk, M. A. & Hutchison, J. L. (1992). *Ultramicroscopy*, **45**, 127–143.
Hall, C. R. & Hirsch, P. B. (1965). *Proc. R. Soc. London Ser. A*, **286**, 158–177.
Humphreys, C. J. (1979). *Rep. Prog. Phys.* **42**, 1825–1887.
Kirkland, E. J. (1984). *Ultramicroscopy*, **15**, 151–172.
Lentzen, M. & Urban, K. (1996). *Ultramicroscopy*, **62**, 89–102.
Lichte, H. (1991). *Advances in Optical and Electron Microscopy*, edited by T. Mulvey & C. J. R. Sheppard, Vol. 12, pp. 25–91. London: Academic Press.
Nellist, P. D., McCallum, B. C. & Rodenberg, J. M. (1995). *Nature (London)*, **374**, 630–632.
Orchowski, A., Rau, W. D. & Lichte, H. (1995). *Phys. Rev. Lett.* **74**, 399–402.

Peng, L.-M. & Wang, S. Q. (1994). *Acta Cryst.* A**50**, 759–771.
Peng, L.-M. & Zuo, J. M. (1995). *Ultramicroscopy*, **57**, 1–9.
Press, W. H., Teukolsky, S. A., Vetterling, W. T. & Flannery, B. P. (1992). *Numerical Recipes in Fortran*, 2nd ed., pp. 375–381. Cambridge University Press.
Rez, P. (1999). *Acta Cryst.* A**55**, 160–167.
Sheinin, S. S. & Jap, B. K. (1979). *Phys. Status Solidi B*, **91**, 407–412.
Sinkler, W. & Marks, L. D. (1999). *Ultramicroscopy*, **75**, 251–268.
Spence, J. C. H. (1993). *Acta Cryst.* A**49**, 231–260.
Spence, J. C. H. (1998). *Acta Cryst.* A**54**, 7–18.
Spence, J. C. H., Calef, B. & Zuo, J. M. (1999). *Acta Cryst.* A**55**, 112–118.
Tonomura, A. (1987). *Rev. Mod. Phys.* **59**, 639–669.
Van Dyck, D. & Coene, W. (1987). *Optik (Stuttgart)*, **77**, 125–128.
Van Dyck, D. & Op de Beeck, M. (1993). *Optik (Stuttgart)*, **93**, 103–107.
Van Dyck, D. & Op de Beeck, M. (1996). *Ultramicroscopy*, **64**, 99–107.
Waasmaier, D. & Kirfel, A. (1995). *Acta Cryst.* A**51**, 416–431.
Zhu, Y. & Tafto, J. (1997). *Philos. Mag.* B**75**, 785–791.
Zou, X., Sunberg, M., Larine, M. & Hovmöller, S. (1996). *Ultramicroscopy*, **62**, 103–121.
Zuo, J. M. (1993). *Ultramicroscopy*, **52**, 459–464.